Lawrence Berkeley Laboratory
UNIVERSITY OF CALIFORNIA

ENERGY & ENVIRONMENT
DIVISION

Submitted to the Journal of Heat Transfer

# HEAT TRANSFER DURING THE SHOCK-INDUCED IGNITION OF AN EXPLOSIVE GAS

H. Heperkan and R. Greif

June 1980



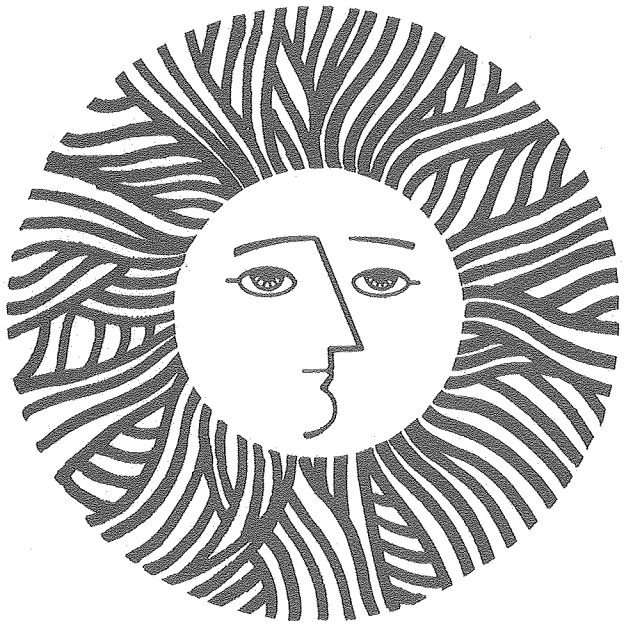



Prepared for the U.S. Department of Energy under Contract W-7405-ENG-48

## DISCLAIMER

# HEAT TRANSFER DURING THE SHOCK-INDUCED IGNITION OF AN EXPLOSIVE GAS

H. Heperkan and R. Greif

University of California, Berkeley
Lawrence Berkeley Laboratory
Energy and Environment Division

and

Department of Mechanical Engineering
Berkeley, California 94720

# ABSTRACT

An experimental and theoretical study has been made of the unsteady heat transfer during the shock-induced ignition of an explosive gas. The heat flux at the end wall is obtained from measurements that were made with a thin film resistance thermometer. A separate analysis is based on the solution of the boundary layer equations in the gas near the end wall. Comparison of these results yields the rate of propagation of the reaction zone towards the wall and the temperature distribution in the gas.

ACKNOWLEDGMENT

It is a pleasure to acknowledge the interest and assistance of Professor A.K. Oppenheim, Dr. L.M. Cohen, K. Hom, A. Shaw and J. Naccache during the course of this research. The work was supported by the Office of Energy Research, Conservation and Solar Energy Division, of the U.S. Department of Energy under Contract No. W-7405-ENG-48.

# INTRODUCTION

This paper reports on an experimental and analytical study of the unsteady heat transfer occurring prior to and during a combustion reaction. The study is made in a shock tube in the region behind the reflected shock wave. Previous shock tube research has emphasized the dynamic effects resulting from the exothermic processes that occur in the course of a combustion reaction [e.g., Oppenheim, Cohen, Short, Cheng and Hom [1]]. The present work utilizes these results as well as the experimentally determined wall heat flux reported herein to model the transport phenomena in the region near the wall. In particular, a thermal boundary layer is assumed which yields the rate of propagation of the reaction zone towards the wall.

The study has been carried out with a mixture of hydrogen and oxygen with argon as the diluent. Reproducibility of the results was demonstrated and a separate study with pure argon was also made.

## EXPERIMENTAL APPARATUS AND MEASUREMENTS

The measurements were made in an aluminum shock tube of rectangular cross-section, 1½" (3.84 cm) by 1-3/4" (4.48 cm). Experiments were carried out with an inert gas, argon, and with a combustible mixture of $2H_2 + O_2 + 27A$ as the test or driven gases on the low pressure side of the diaphragm. The driver gas, on the high pressure side, was helium.

Two Kistler pressure transducers (S/N 52036) were mounted on the top of the test (or expansion) section to detect the arrival of the shock wave at their respective locations. The resulting signals were recorded on a Tektronix dual beam oscilloscope. The transducers were placed 4.00" (10.16 cm) apart. The travel time of the shock wave between the pressure transducers was determined from measurements made with a Hewlett-Packard electronic digital counter. From these measurements the speed of the shock wave was determined. The sound speed was determined from the measurement of the initial temperature of the test gas. The resulting values of the Mach number, along with the initial temperature and pressure, permit the calculation of the temperature and the pressure behind the incident shock wave and behind the shock wave that reflects off the end wall.

To measure the temperature at the end wall as a function of time, a thin-film resistance thermometer was used [2-12]. This gauge consisted of a thin platinum film that was painted and baked on a ceramic base, Macor, made by Corning Glass Works. The gauge was mounted flush with the wall. A temperature change caused a change in the resistance of the platinum film and the corresponding voltage was recorded (cf. Fig. 1). The resistance thermometer was calibrated in a thermally controlled enclosure so that the wall temperature variation could then be determined from the voltage output. The value of the

resulting heat flux is dependent on the parameter $(\rho ck)^{\frac{1}{2}}$ of the insulating ceramic base. This value is 0.033 cal/cm$^2$ °Cs$^{\frac{1}{2}}$ (0.138 Ws$^{\frac{1}{2}}$/cm$^2$K) for Macor [11,12].

Measurements with the combustible mixture [$2H_2 + O_2 + 27A$] were carried out for two nominally identical runs: 214 and 219, corresponding to initial pressures of 1.84 psia (95.2 mm Hg) and 1.85 psia (95.4 mm Hg); initial temperatures of 534.5°R (296.9°K) and 535.1°R (297.3°K); Mach numbers of 2.35 and 2.39. The values of the pressure and the temperature immediately after shock wave reflection are 44.9 psia (2322 mm Hg) and 47.3 psia (2445 mm Hg); 2371°R (1317°K) and 2407°R (1337°K).

## ANALYSIS

The determination of the heat flux during shock wave heating is based on the measured surface temperature of a thermally infinite solid (Macor) that is initially at a constant temperature. The solution for the wall heat flux is given by [5]:

$$q_{ws} = \left(\frac{k\rho c}{\pi}\right)_s^{\frac{1}{2}} \int_0^t \frac{1}{(t-\bar{t})^{\frac{1}{2}}} \frac{dT_w}{d\bar{t}}\, d\bar{t} \tag{1}$$

To perform the numerical calculations for the heat flux it is more convenient to use the following form of equation (1) [5]:

$$q_{ws} = \left(\frac{k\rho c}{\pi}\right)_s^{\frac{1}{2}} \left\{\frac{T_w(t)-T_i}{t^{\frac{1}{2}}} + \frac{1}{2}\int_0^t \frac{T_w(t)-T_w(\bar{t})}{(t-\bar{t})^{3/2}}\, d\bar{t}\right\} \tag{2}$$

which does not involve the evaluation of derivatives.

In the absence of combustion the end wall temperature rapidly increases to a value $T_w$ that remains constant [5]. For this condition the wall heat flux is given by

$$q_{ws} = \left(\frac{k\rho c}{\pi}\right)_s^{\frac{1}{2}} \frac{T_w-T_i}{t^{\frac{1}{2}}} \tag{3}$$

An alternative evaluation of the wall flux may be obtained from a solution of the conservation equations in the gas. The gas in the end wall region undergoes a rapid increase in temperature due to compression from both the incident and the reflected shock waves. The effect of the wall is to cool the gas in a boundary layer which grows with time. Neglecting viscous dissipation and species diffusion and taking the pressure to be

uniform yields the following one-dimensional equations of continuity and energy [6-9]:

$$\frac{\partial \rho}{\partial t} + \frac{\partial}{\partial x}(\rho u) = 0 \tag{4}$$

$$\rho\, c_p \frac{\partial T}{\partial t} + \rho u\, c_p \frac{\partial T}{\partial x} = \frac{dp}{dt} + \frac{\partial}{\partial x}\left(k \frac{\partial T}{\partial x}\right) \tag{5}$$

where x is the coordinate perpendicular to the end wall. The continuity equation is satisfied by a stream coordinate $\psi$ according to

$$\frac{\partial \psi}{\partial x} = \frac{\rho}{\rho_{ig}} \quad , \qquad \frac{\partial \psi}{\partial t} = -\frac{\rho u}{\rho_{ig}} \tag{6}$$

where $\rho_{ig}$ is the initial constant density of the gas after shock wave reflection. The energy equation in $\psi$,t coordinates is then given by

$$\rho\, c_p \frac{\partial T}{\partial t} = \frac{dp}{dt} + \frac{\rho}{\rho_{ig}} \frac{\partial}{\partial \psi}\left(k \frac{\rho}{\rho_{ig}} \frac{\partial T}{\partial \psi}\right) \tag{7}$$

During the pre-ignition period, corresponding to about the first twenty microseconds after the shock wave has reflected off the end wall, the pressure is constant and results for the heat transfer may be readily obtained. This interval is followed by ignition which takes place in a plane close to the end wall. This is accompanied by a detonation wave which propagates away from the end wall and a diffusion transport which proceeds towards the wall. In view of the different phenomena occurring in the preignition and combustion periods, it is convenient to consider them separately.

Pre-Ignition Period

During this interval the pressure is constant and the analysis is identical to that for an inert gas [6-9]. Briefly, the energy equation becomes:

$$\frac{1}{\alpha_{ig}} \frac{\partial \theta}{\partial t} = \frac{\partial}{\partial \psi} \left[ \frac{K}{\theta} \frac{\partial \theta}{\partial \psi} \right] \tag{8}$$

where

$$\theta = T/T_{ig}, \quad T_{ig} = T_{\infty} = T_5^*, K = k/k_{ig}, \quad \alpha_{ig} = k_{ig}/\rho_{ig} c_p$$

Note that for an ideal gas at constant pressure $\rho/\rho_{ig} = T_{ig}/T = 1/\theta$. The initial and boundary conditions are:

$$T(\psi,0) = T_{ig} \quad , \quad T(0,t) = T_w \quad , \quad T(\infty,t) = T_{ig} \tag{9}$$

The end wall location corresponds to $\psi = 0$.

Since there is no characteristic length or time in the problem, it is apparent that $\theta$ is a function only of $\psi^2/\alpha_{ig} t$ [6-9]. This requires that the wall surface temperature, $T_w$, be a constant which is in agreement with the experimental results [6-9]. Therefore we let $\eta = \psi/(2\alpha_{ig} t)^{\frac{1}{2}}$ and obtain

---

*$T_{ig}$ is the temperature of the gas immediately after the shock wave has reflected off the end wall (Liepmann and Roshko [13]). The subscript ig is used to distinguish this from the initial (room temperature) condition in the solid as used in Eqs. (2) and (3).

$$\frac{d}{d\eta}\left(\frac{K(\theta)}{\theta}\frac{d\theta}{d\eta}\right) + \eta\frac{d\theta}{d\eta} = 0 \tag{10}$$

$$\theta(0) = 1\ , \quad \theta(\infty) = \frac{T_\infty}{T_w} = \frac{T_{ig}}{T_w} \tag{11}$$

Using a power law dependence for the thermal conductivity, $K = k/k_{ig} = (T/T_{ig})^a$, with a value for a, completes the specification of the problem [ 8,9 ]. For a = 1.0 the heat flux obtained from Eqs. (10) and (11) is given by

$$q_{wg} = k_{ig}\frac{(T_\infty - T_w)}{\sqrt{\pi\,\alpha_{ig}\,t}} \tag{12}$$

This result is also given in the Appendix. For a equal to 0.7 [8,9,14] the heat flux $q_{wg}$ is obtained from a numerical solution to Eq. (10) subject to Eq. (11) [8,9].

Combustion Period

The next interval includes the effects of combustion and now the pressure is time dependent. The energy equation in $\psi$,t coordinates is now given by

$$\frac{\partial T}{\partial t} = \frac{\gamma-1}{\gamma}\frac{T}{p}\frac{dp}{dt} + \alpha_{ig}\frac{p}{p_{ig}}T_{ig}^{1-a}\frac{\partial}{\partial\psi}\left(T^{a-1}\frac{\partial T}{\partial\psi}\right) \tag{12}$$

Introducing

$$V = \left(\frac{T}{T_{ig}}\right)^{a}\left(\frac{p}{p_{ig}}\right)^{a(1-\gamma)/\gamma} \quad \text{and} \quad d\tau = \left(\frac{p}{p_{ig}}\right)^{(a\gamma-a+1)/\gamma} dt \tag{13}$$

yields

$$\frac{\partial V}{\partial \tau} = \alpha_{ig} V^{\frac{a-1}{a}}\frac{\partial^2 V}{\partial \psi^2} \tag{14}$$

The initial and boundary conditions are:

$$V(\psi,\tau_I) = fcn(\psi) \tag{15a}$$

$$V(0,\tau) = \left(\frac{T_w}{T_{ig}}\right)^{a}\left(\frac{p}{p_{ig}}\right)^{a(1-\gamma)/\gamma} \tag{15b}$$

$$V(\delta,\tau) = \left(\frac{T_c}{T_{ig}}\right)^{a}\left(\frac{p}{p_{ig}}\right)^{a(1-\gamma)/\gamma} \tag{15c}$$

The transformed time $\tau_I$ is defined to be the time at the beginning of the combustion period which is the same as the time at the end of the pre-ignition period. The temperature of the combustion zone, $T_c$, along with the location of the combustion zone, $\delta$, are required and these are discussed in the next section. For completeness it is noted that Eq. (14) was solved numerically using an explicit finite difference method to calculate the temperature profiles and the heat flux $q_{wg}$. A time increment, $\Delta\tau$, of 1$\mu$ second and a space increment, $\Delta\psi$, of 15.1$\mu$ were used.

## RESULTS AND DISCUSSION

It is important to emphasize that the determination of the wall heat flux, $q_{ws}$, only requires the specification of the thermal properties of the ceramic solid and the temperature difference, $T_w - T_i$, in the solid. During the pre-ignition period the wall temperature is constant and the heat flux, $q_{ws}$, is then obtained from the simple relation, Eq. (3).

The determination of the heat flux, $q_{wg}$, during the pre-ignition period was previously presented [cf. Pre-Ignition Period, Eqs. (8) - (12)]. Briefly, during this period the pressure, p, the wall temperature, $T_w$, and the temperature outside the boundary layer, $T_\infty$, are constant and the phenomena and analysis are identical to that for the inert gas problem [6-9]. The heat transfer, $q_{wg}$, is determined from the solution of the energy equation, Eq. (10), subject to the conditions of Eq. (11). A comparison of the values obtained for the heat fluxes, $q_{wg}$, with a = 0.7 and a = 1.0* [8,9,14] and, $q_{ws}$, as obtained from Eq. (3) is presented in Figs. 2a and 2b. During the pre-ignition period, which corresponds to the first 20 μsec after shock wave reflection, the heat fluxes agree to within 4% and 6% for Figs. 2a and 2b, respectively. For runs with pure argon the agreement was 8% and 3% for two runs.

Recall that during the pre-ignition period the pressure is constant so that $\tau = t$. The heat flux decreases during this interval because the temperature difference across the thermal boundary layer in the gas, $T_\infty - T_w$, is constant while the thickness of the layer is increasing with time. The heat fluxes in Figs. 2a and 2b show this decrease during the pre-ignition period.

---

*The result for a = 1.0 is discussed in the Appendix.

When combustion begins, the temperature of the gas in the reaction zone rapidly increases and this effect diffuses to the end wall where it increases the wall temperature (cf. Fig. 1) and increases (or retards the rate of decrease of) the wall flux. This variation of the heat flux, $q_{ws}$, is shown in Figs. 2a and 2b.

The determination of the heat flux, $q_{wg}$, requires information relevant to the gas transport. From the work of Oppenheim, et al. [1], Cohen, et al. [15-17], and Cheng [18] the induction or "ignition" time* is 20 μsec after the shock wave has reflected off the end wall. The reaction is initiated at this time and is assumed to take place at the penetration depth or boundary layer thickness, $\delta$; i.e., the location where the temperature reaches 99 percent of the free stream value. From the analysis during the pre-ignition period the penetration depth and the temperature distribution are determined as a function of time and at $\tau = \tau_I = 20$ μsec this gives the initial condition for the combustion period required in Eq. (15a). The calculations of the pressure, p, and the temperature of the reaction zone, $T_c$, during the course of the reaction were based on previous experiments and theoretical studies which included the gas dynamic phenomena and the chemical kinetics of the reaction [1,15-18]. The values are shown in Figs. 3 and 4 for Run 214 and the values of $\tau$ are given in Table 1. The remaining consideration is the propagation of the reaction zone, $\delta(t)$. Once this quantity is obtained the energy transfer may be determined in accordance with the solution of Eq. (14) subject to Eqs. (15). Note that the model is one of thermal transport with the effect of combustion to increase the temperature of the reaction zone.

Calculations were made for different trajectories for the reaction zone, $\delta(t)$, as shown in Figs. (5a) and (5b) and the corresponding values that

*This is designated as the pre-ignition period.

were calculated for $q_{wg}$ are shown in Fig. 6 for Run 214. The diffusion from the reaction zone to the wall proceeds in the same manner for all the cases considered; the difference is solely that the propagation is stopped at a final or quenching distance at $\psi_{BF} = 9\Delta\psi$, $8\Delta\psi$, $7\Delta\psi$ or $6\Delta\psi$ ($\Delta\psi = 15.1\ \mu$) for the various cases considered. The calculations were carried out with the temperature, $T_c$, at the same location for two consecutive time increments. In detail, for Run 214, values of $T_c$ equal to 1338°K and 1339°K were applied at 196μ for two consecutive time steps; $T_c$ = 1342°K and 1343°K were applied at 181μ for the next two consecutive time steps, etc. From the comparison of the fluxes, $q_{ws}$ and $q_{wg}$, it is seen that the best agreement is achieved for the case $\psi_{BF} = 6\Delta\psi$ and the corresponding temperature distribution in the gas is shown at different times in Fig. 7. Carrying out the transformation from $\psi$ to x yielded the results shown in Figs. 5a and 5b. For the case $\psi_{BF} = 6\Delta\psi$, the minimum value for $\delta$ for Run 214 is 44μ which increases slightly to 50μ at 45 μsec (cf. Fig. 5a). This procedure was also carried out for the nominally identical Run 219 which was cited in the section on Experimental Apparatus and Measurements. For this case the minimum value for $\delta$ is 48μ which increases to 59μ at 45 μsec (cf. Fig. 5b). Calculations were carried out until $\tau$ = 45 μsec. At this time the detonation wave overtakes the reflected shock wave and values for the state of the gas were not available.

For clarification the case $\psi_{BF} = 6\Delta\psi$ is presented separately in Fig. 8a for Run 214 and in Fig. 8b for Run 219. For completeness, the thermal conductivity variation $k/k_{ig} = (T/T_{ig})^1$, i.e., a = 1, is also shown which was discussed in the Appendix.

Of particular interest is the result for the variation of the heat transfer coefficient, h, which is defined by

$$h = \frac{q_w}{T_\infty - T_w} \tag{17}$$

The results for h are presented in Fig. 9 with $h_s$ based on $q_{ws}$ and $h_g$ based on $q_{wg}$. The heat transfer coefficient decreases during the pre-ignition period corresponding to the increase in the thickness of the boundary layer and the constant value for the temperature difference, $T_\infty - T_w$. During the combustion period the heat transfer coefficient decreases slightly and then increases as the effects of combustion diffuse to the end wall. The results for Run 219 are very close to those for Run 214 and are not shown.

In concluding, we note that it would have been desirable to carry out a study over a range of conditions, but this was not feasible because the related information that is required was not available. Indeed, the experimental and theoretical study of the gas dynamics and chemical kinetics of the hydrogen-oxygen system which were needed for the conditions studied in this work represented a substantial portion of the previous work that has been cited [1,15-18]. The present work uses and extends these studies to include transport phenomena in the region near the wall. In particular, results have been presented for the first time for the wall heat flux and the location of the combustion zone as a function of time.

## APPENDIX

For a linear variation of the thermal conductivity with respect to temperature, $K = k/k_{ig} = (T/T_{ig})^a$, $a = 1.0$, Eq. (10) becomes

$$\frac{d^2\theta}{d\eta^2} + n\frac{d\theta}{d\eta} = 0 \tag{A-1}$$

subject to the conditions given in Eq. (11). This linear problem may be readily solved and the result for the heat flux is

$$q_{wg} = k_{ig}\frac{(T_\infty - T_w)}{\sqrt{\pi\,\alpha_{ig}\,t}} \tag{A-2}$$

During the combustion period, the energy equation, Eq. (14), reduces to

$$\frac{\partial V}{\partial \tau} = \alpha_{ig}\frac{\partial^2 V}{\partial \psi^2} \tag{A-3}$$

subject to the conditions

$$V(\psi,\tau_I) = fcn(\psi) \tag{A-4a}$$

$$V(0,\tau) = \left(\frac{T_w}{T_{ig}}\right)\left(\frac{P}{P_{ig}}\right)^{(1-\gamma)/\gamma} \tag{A-4b}$$

$$V(\delta,\tau) = \left(\frac{T_c}{T_{ig}}\right)\left(\frac{P}{P_{ig}}\right)^{(1-\gamma)/\gamma} \tag{A-4c}$$

This problem has been solved numerically.

The case a = 0.7 corresponds to the correct thermal conductivity variation and the better agreement shown in Figs. 2a and 2b for a = 0.7 rather than 1.0 is in accord with this specification. The a = 1.0 case is appealing, however, because the resulting equations are simpler and the corresponding results, although not as accurate as those for the a = 0.7 case, are much more easily obtained and may be adequate for many applications.

## REFERENCES


1. Oppenheim, A.K., Cohen, L.M., Short, J.M., Cheng, R.K. and Hom, K., "Dynamics of the Exothermic Process in Combustion," 15th Symposium (International) on COmbustion, Tokyo, 1974, pp. 1503-1513.

2. Vidal, R., "Model Instrumentation Techniques for Heat Transfer and Force Measurements in a Hypersonic Shock Tunnel," Report AD 917-A-1, Buffalo, N.Y., Cornell Aeronautical Laboratory, Inc., 1956.

3. Rabinowicz, J., Jessey, M.E., and Bartsch, C.A., "Resistance Thermometer for Heat Transfer Measurement in a Shock Tube," GALCIT Hypersonic Research Project Memo, 33, Guggenheim Aeronautical Laboratory, California Institute of Technology, July 1956.

4. Rose, P.H., and Stark, W.I., "Stagnation Point Heat Transfer Measurements in Air at High Temperature," Research Note 24, Everett, Mass., AVCO Research Laboratory, AVCO Manufacturing Corp., December 1956.

5. Hall, J.G., and Hertzberg, A., "Recent Advances in Transient Surface Temperature Thermomentry," Jet Propulsion, Vol. 28, 1958, pp. 719-723.

6. Camac, M., Fay, J.A. Feinberg, R.M., and Kemp, N.H., Heat Transfer from High Temperature Argon, p. 58. Proceedings of the 1963 Heat Transfer and Fluid Mechanics Institute, Stanford University Press, California (1963).

7. Lauver, M.R., Shock Tube Thermal Conductivity, Phys. Fluids 7, 611 (1964).

8. Collins, D.J., Greif, R., and Bryson, A.E., "Measurements of the Thermal COnductivity of Helium in the Temperature Range 1600-6700 K," Int. J. Heat Mass Transfer, Vol. 8, 1965, pp. 1209-1216.

9. Collins, D.J., "Shock Tube Study for the Determination of the Thermal Conductivity of Neon, Argon, and Krypton," ASME Journal of Heat Transfer, Vol. 88, 1966, pp. 52-56.

10. Isshiki, N., and Nishiwaki, N., "Study on Laminar Heat Transfer of Inside Gas with Cyclic Pressure Change on an Inner Wall of a Cylinder Head," 4th International Heat Transfer Conference, Paris-Versialles, 1970, FC 3.5, pp. 1-10.

11. Nikanjam, M., and Greif, R., Heat Transfer During Piston Compression, J. Heat Transfer 100, 527-530 (1978).

12. Greif, R., Namba, T., and Nikanjam, M., "Heat Transfer during Piston Compression Including Side Wall and Convection Effect," Int. J. Heat Mass Transfer, 22, 1979, pp. 901-907.

## LIST OF FIGURES



## TABLE

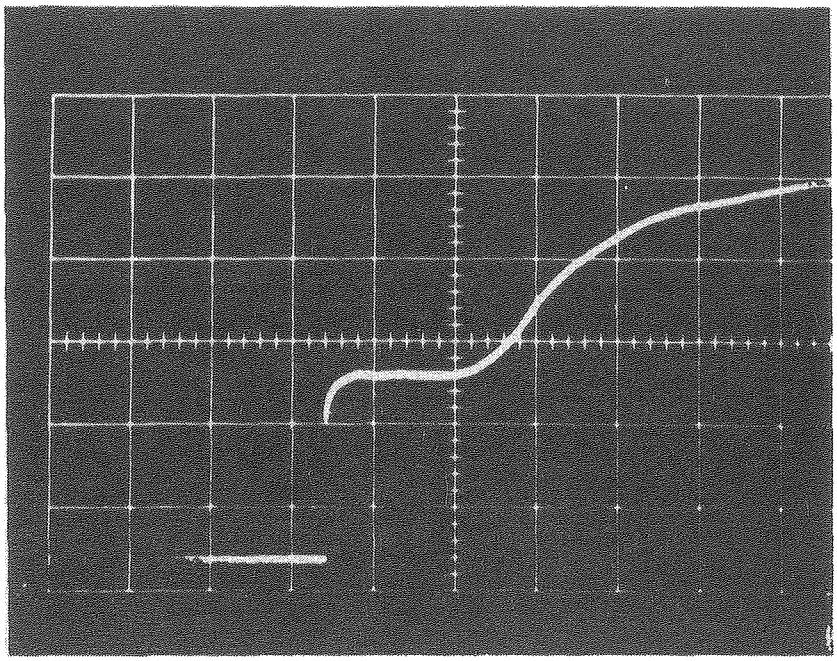

XBB 806-7216

Fig. 1

SURFACE TEMPERATURE MEASUREMENT,
REACTING GAS

TIME SCALE = 20 $\mu$ sec/cm
PRE—IGNITION TEMP. INCREASE =
4.6°K = 8.3°R
$2H_2 + O_2 + A$, RUN 214

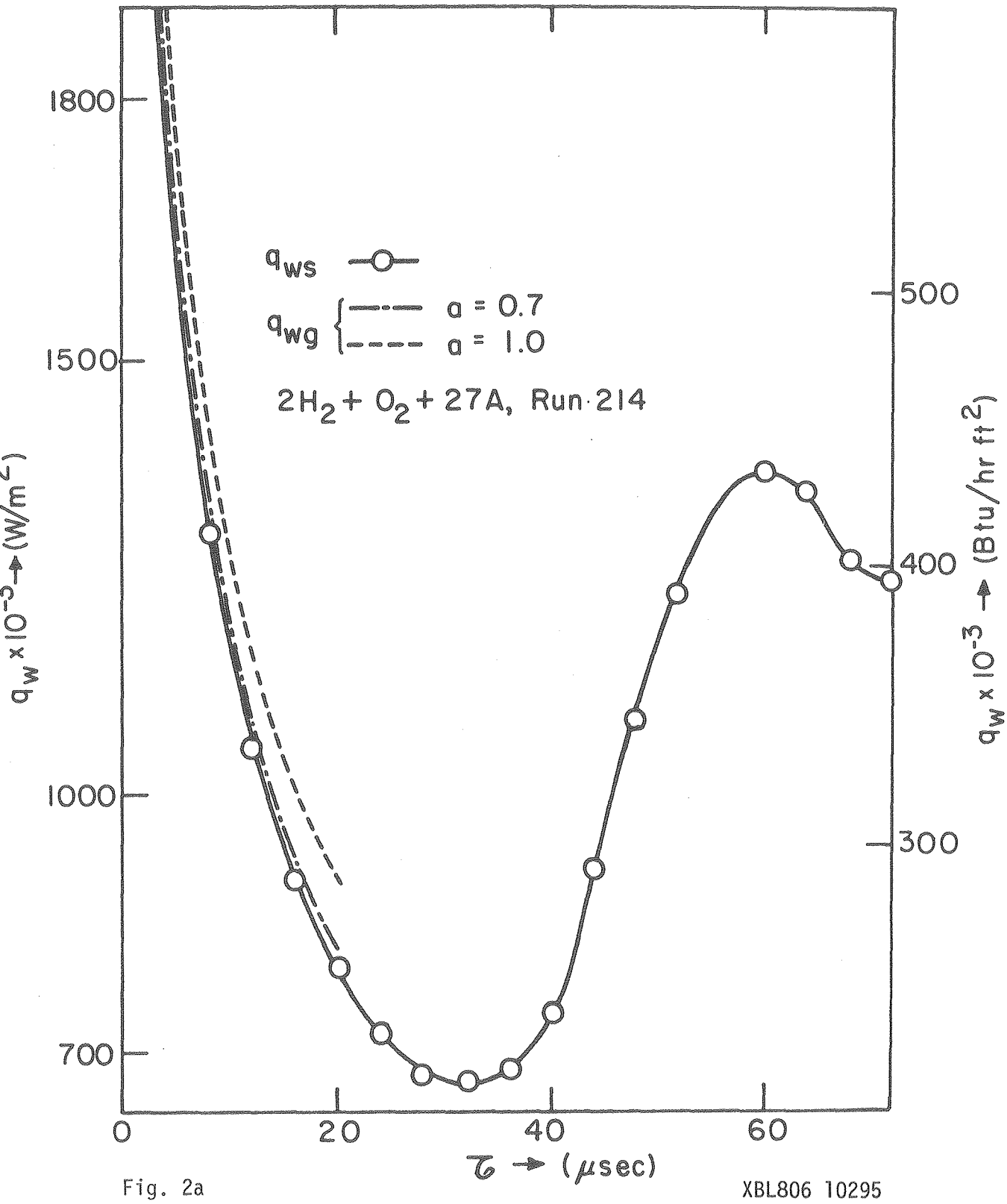


Fig. 2a

XBL806 10295

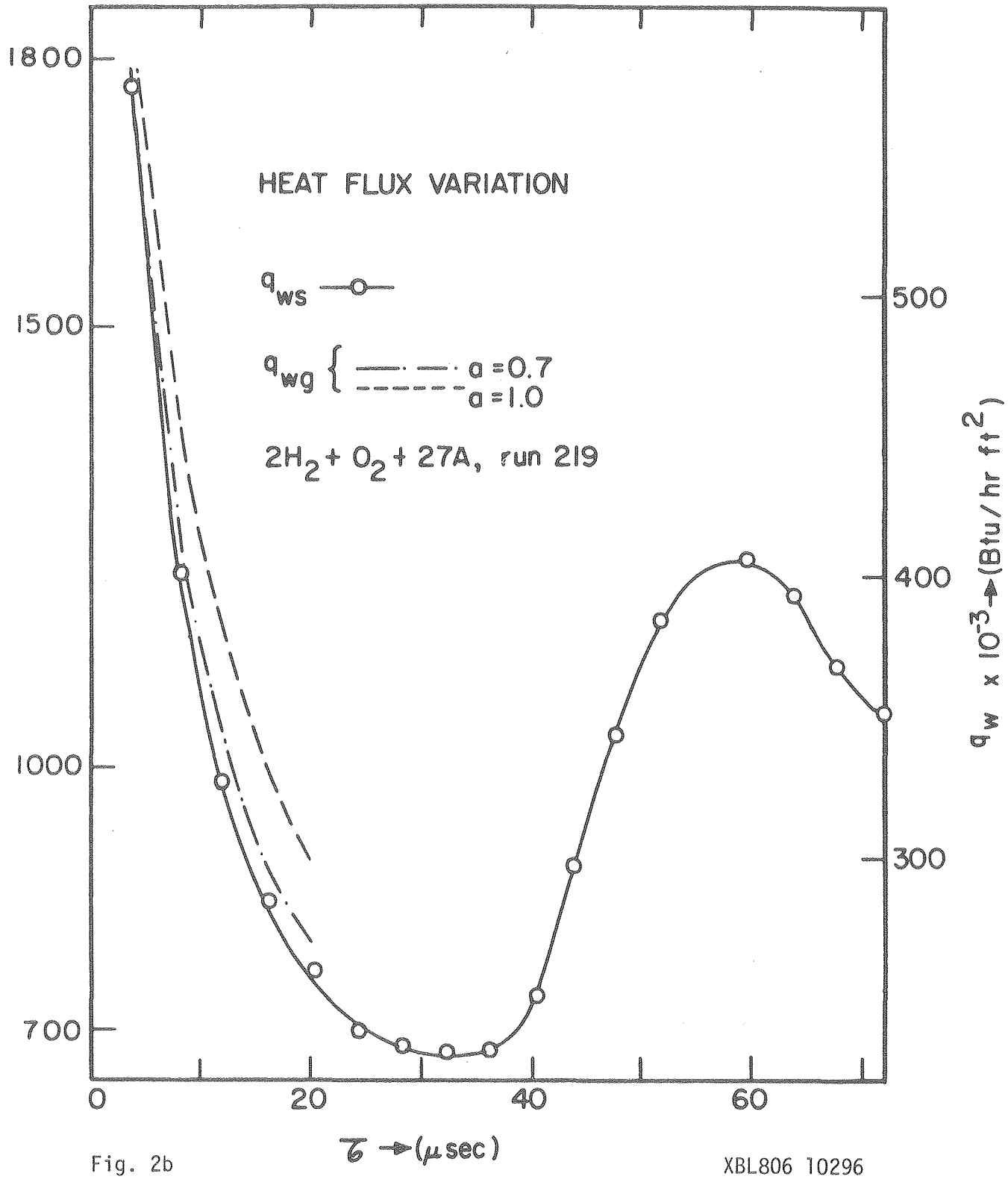


Fig. 2b

XBL806 10296

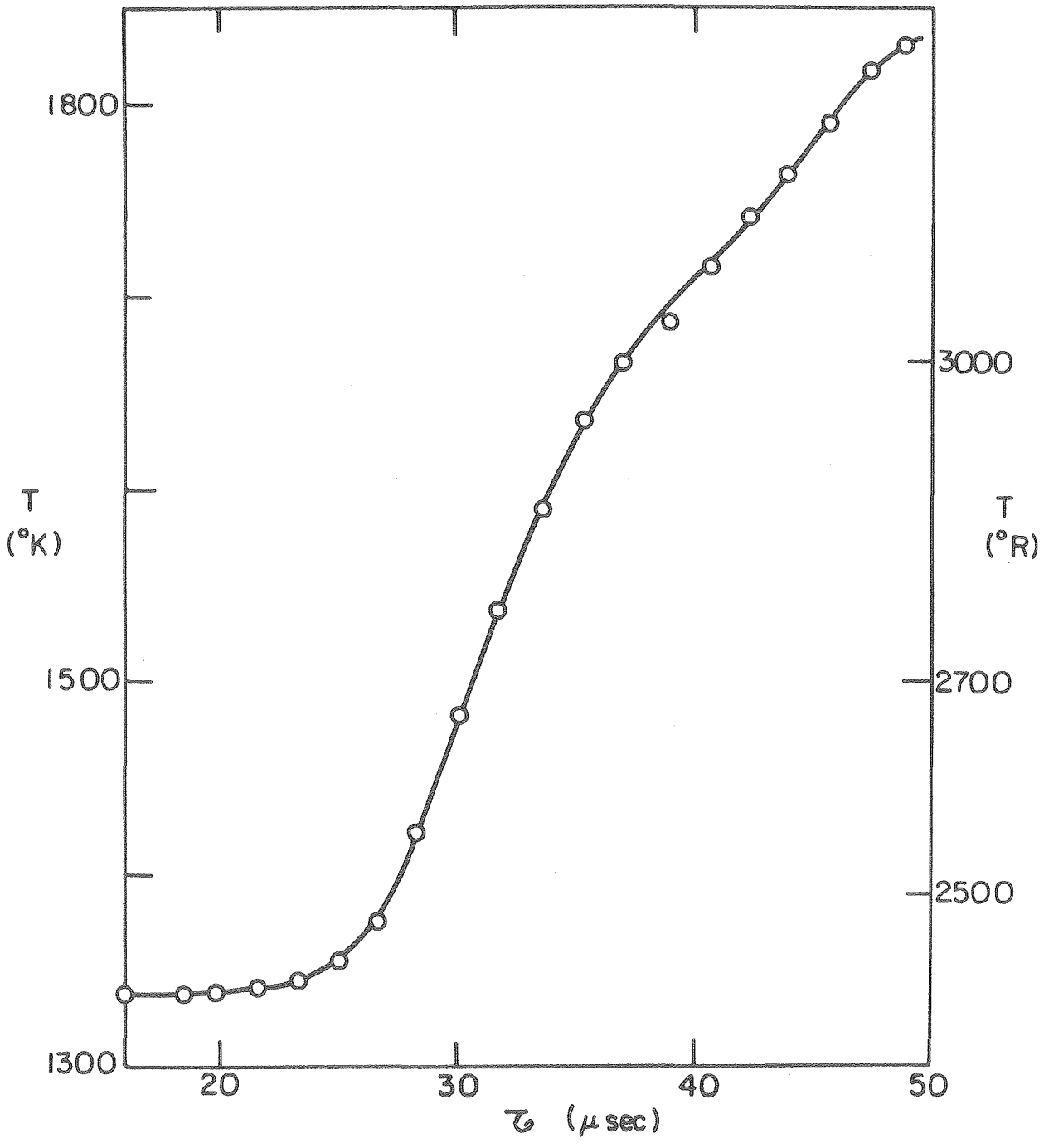


Fig. 3

XBL806 10297

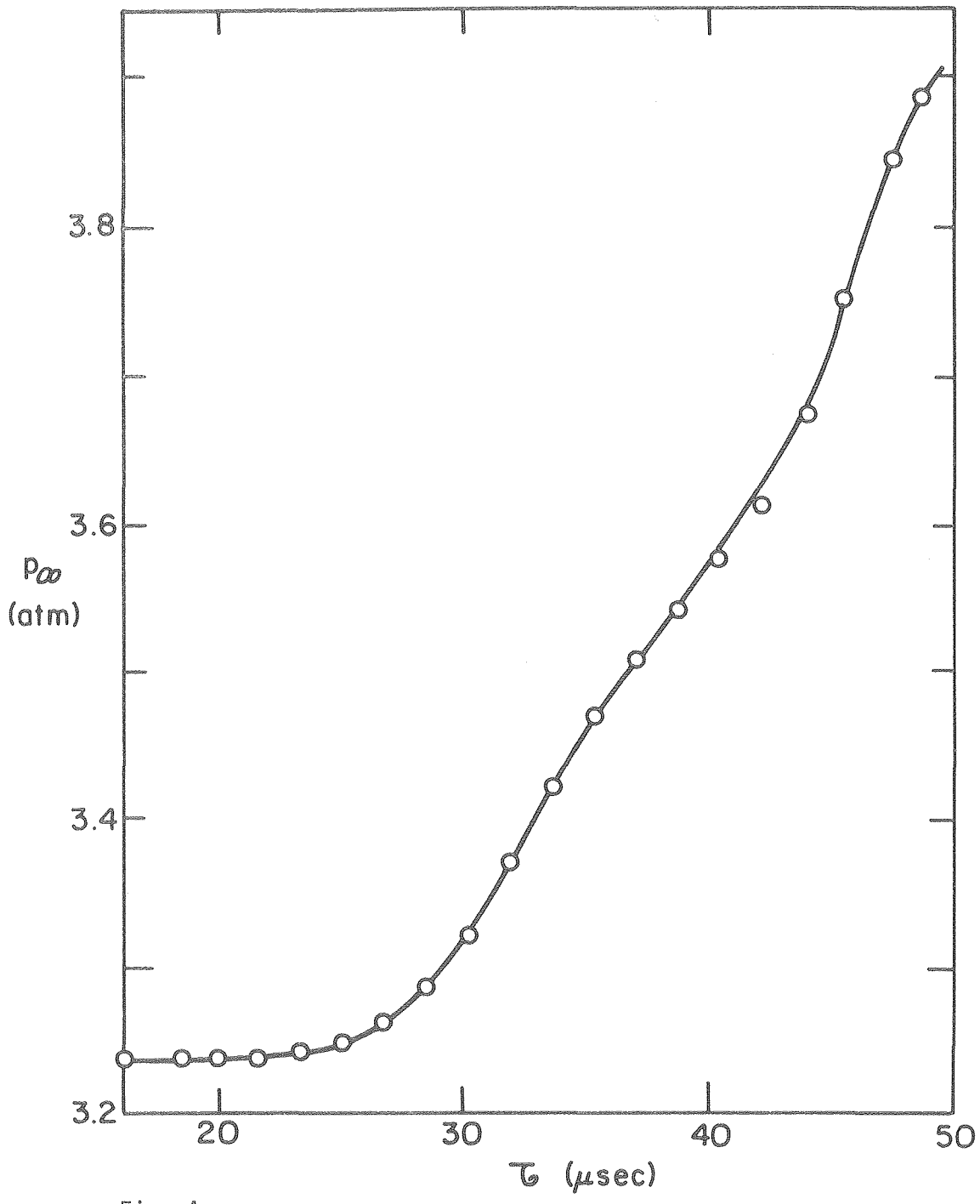


Fig. 4

XBL806 10298

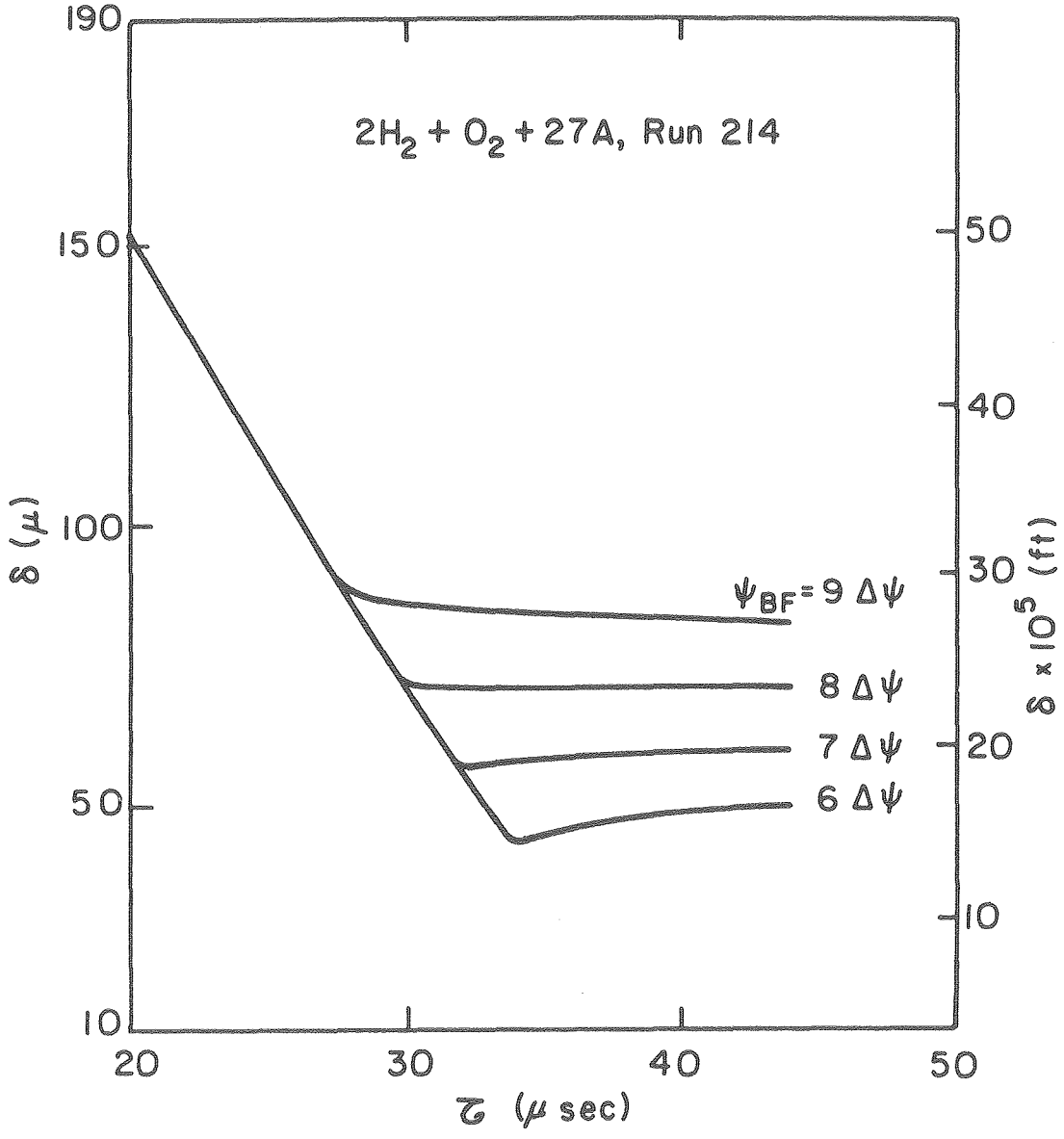


Fig. 5a

XBL806 10299

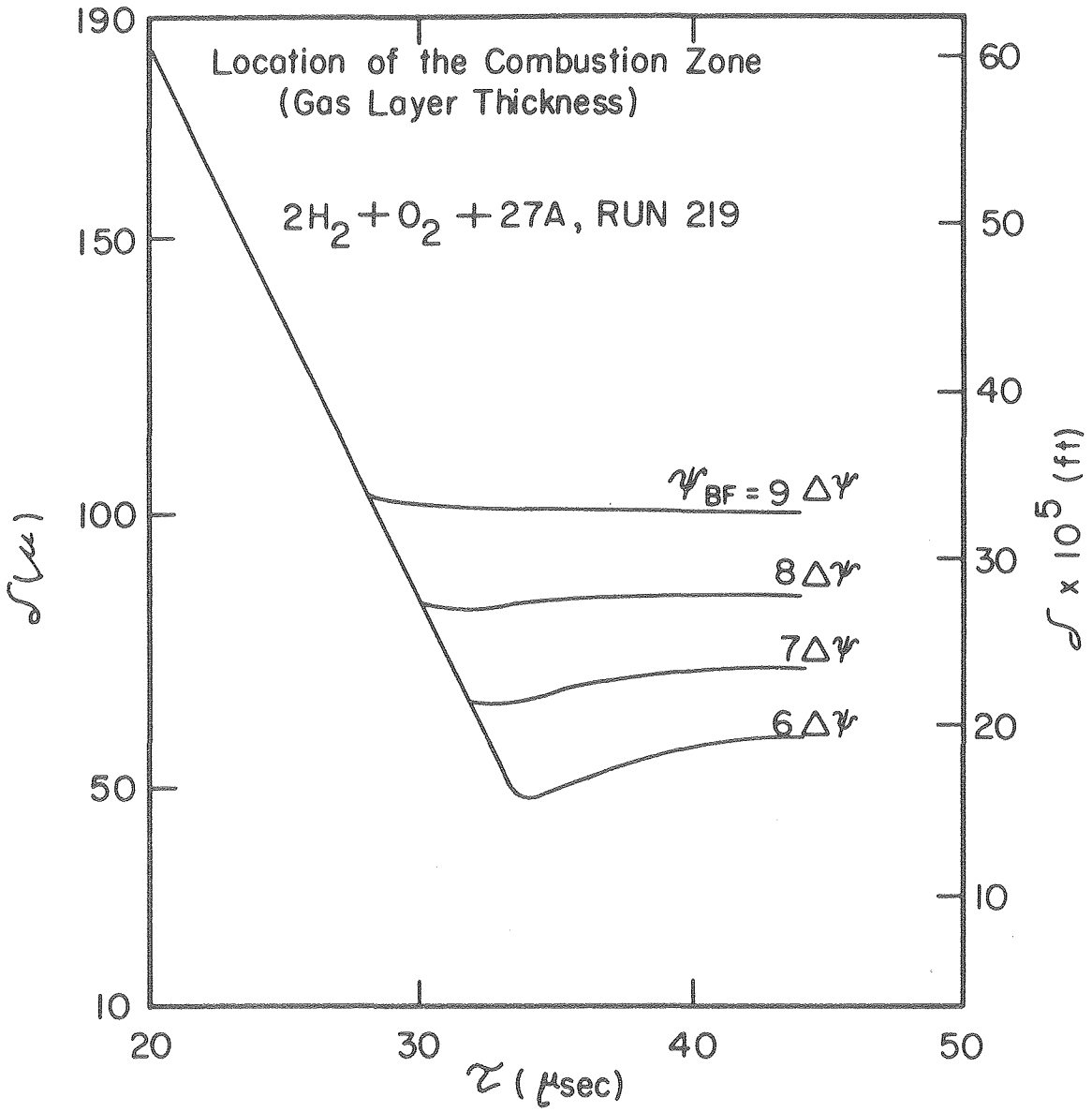


Fig. 5b

XBL806 10300

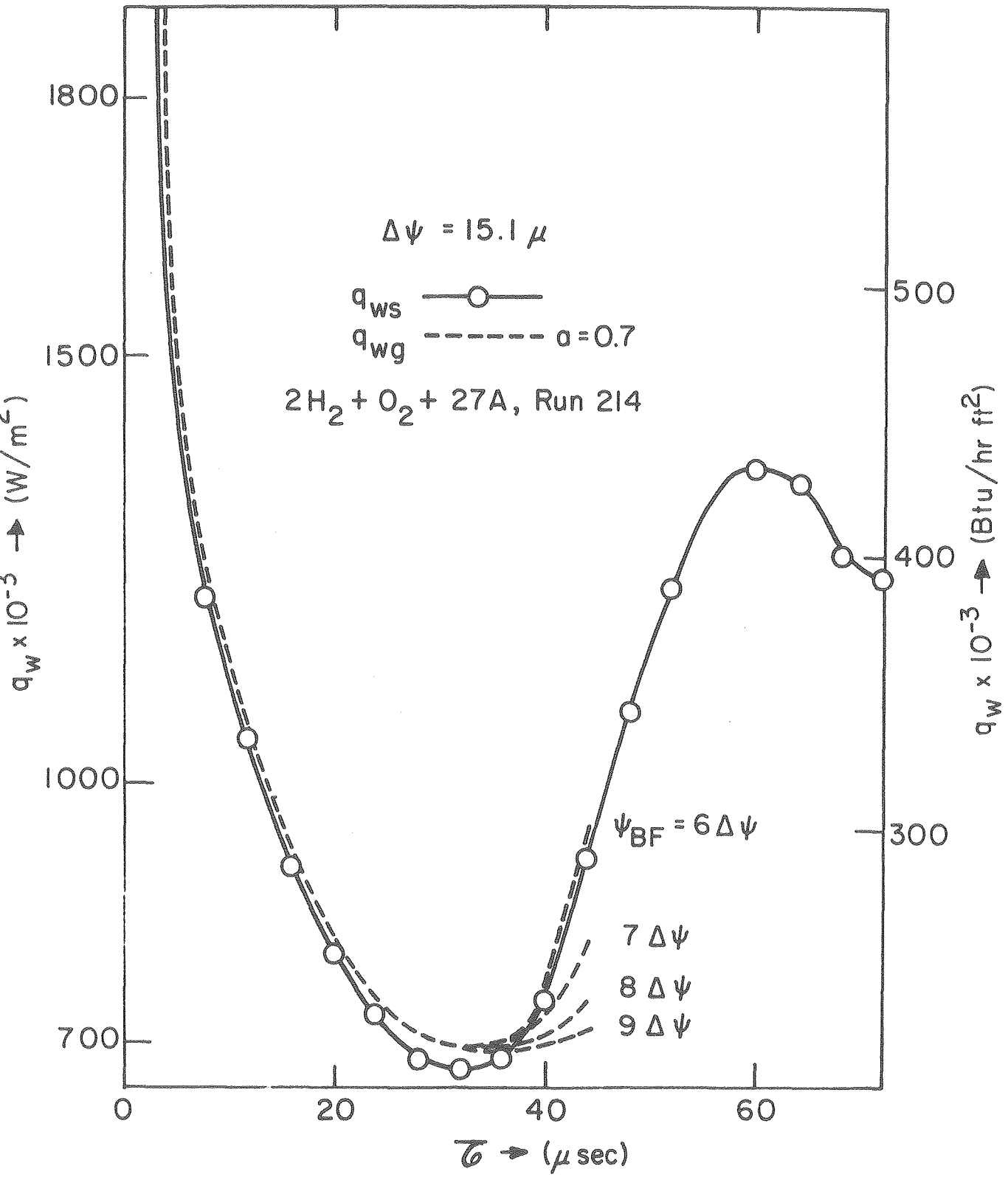


Fig. 6

XBL806 10301

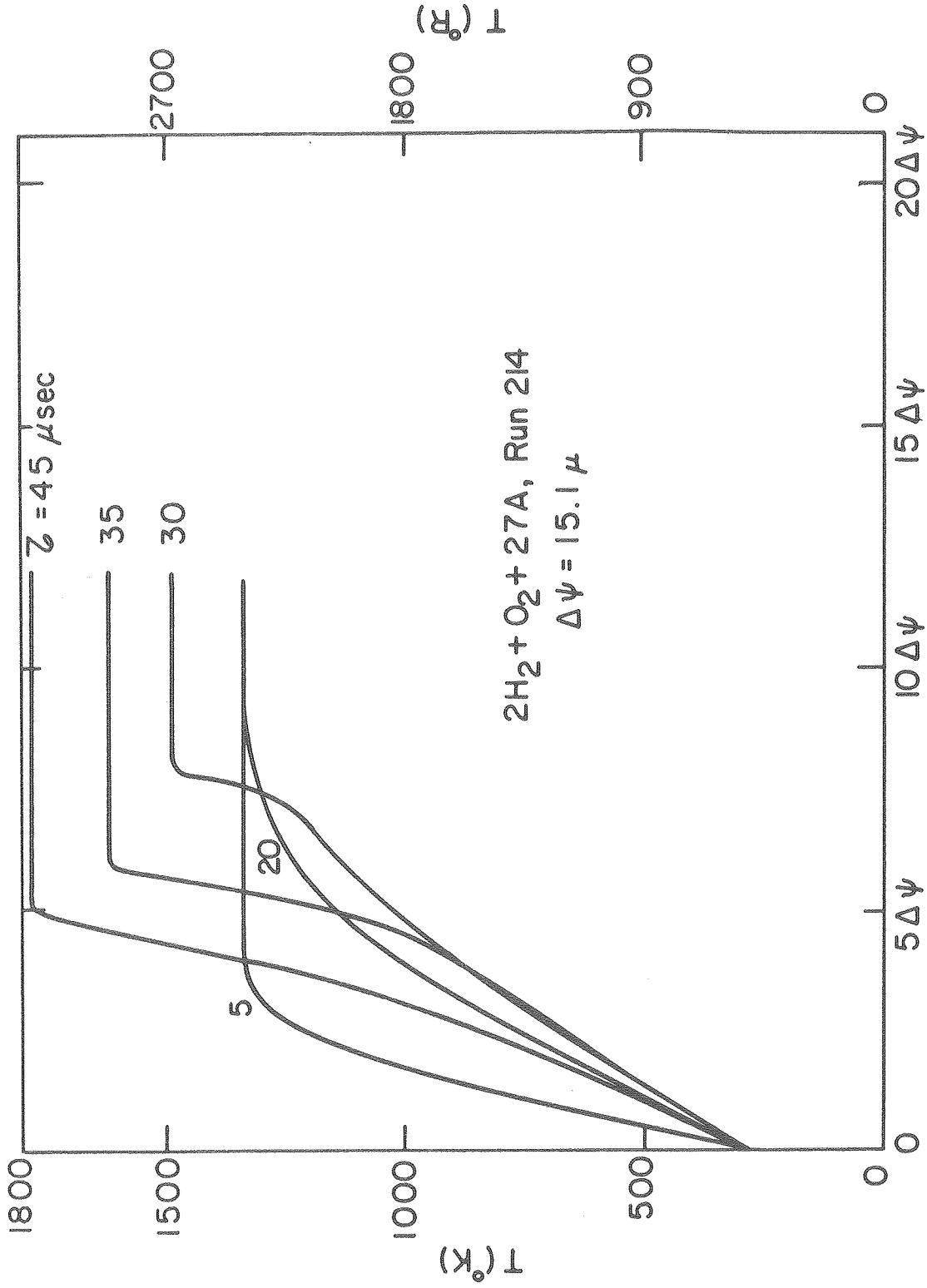


XBL806 10302

Fig. 7

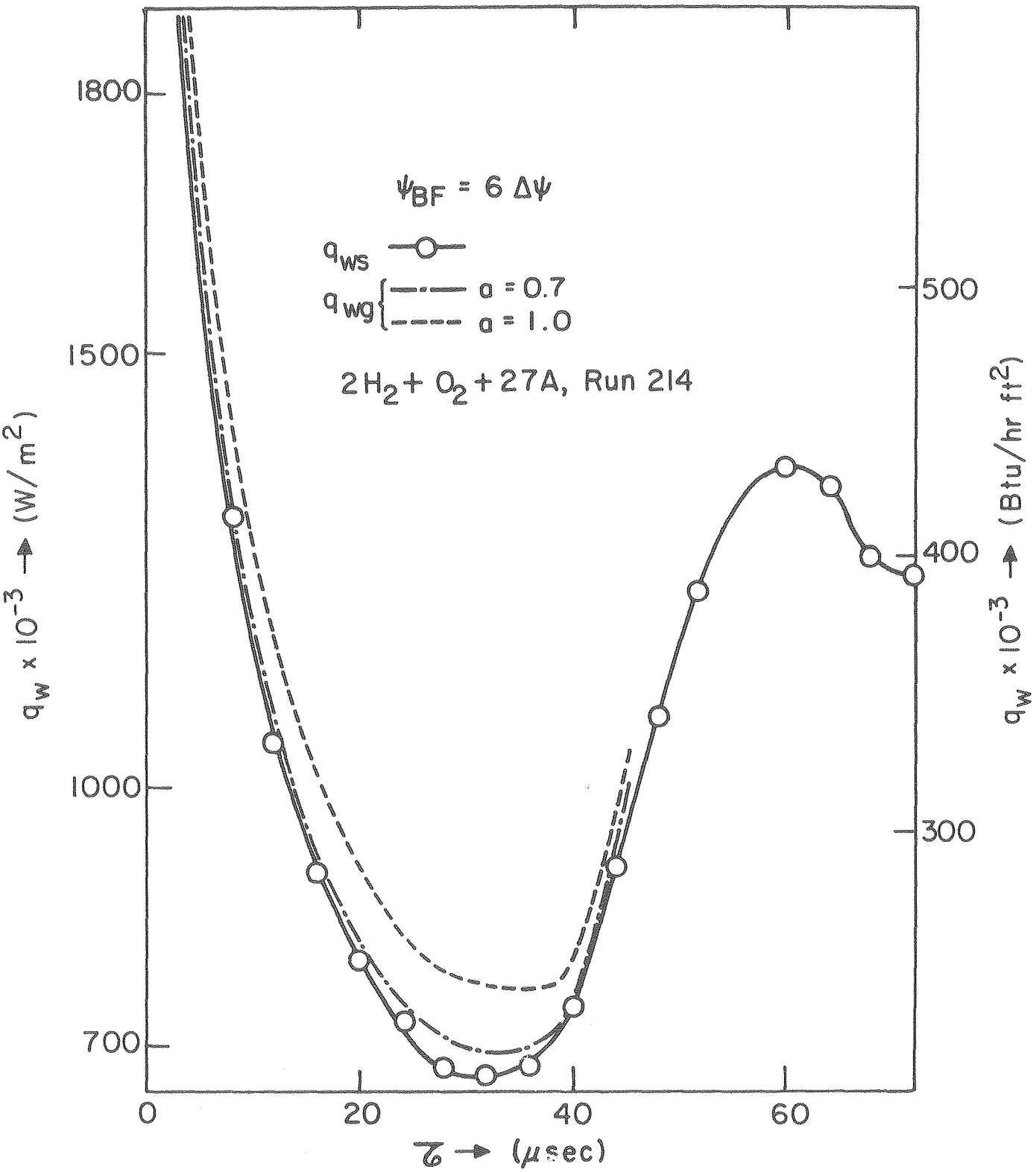


Fig. 8a

XBL806 10303

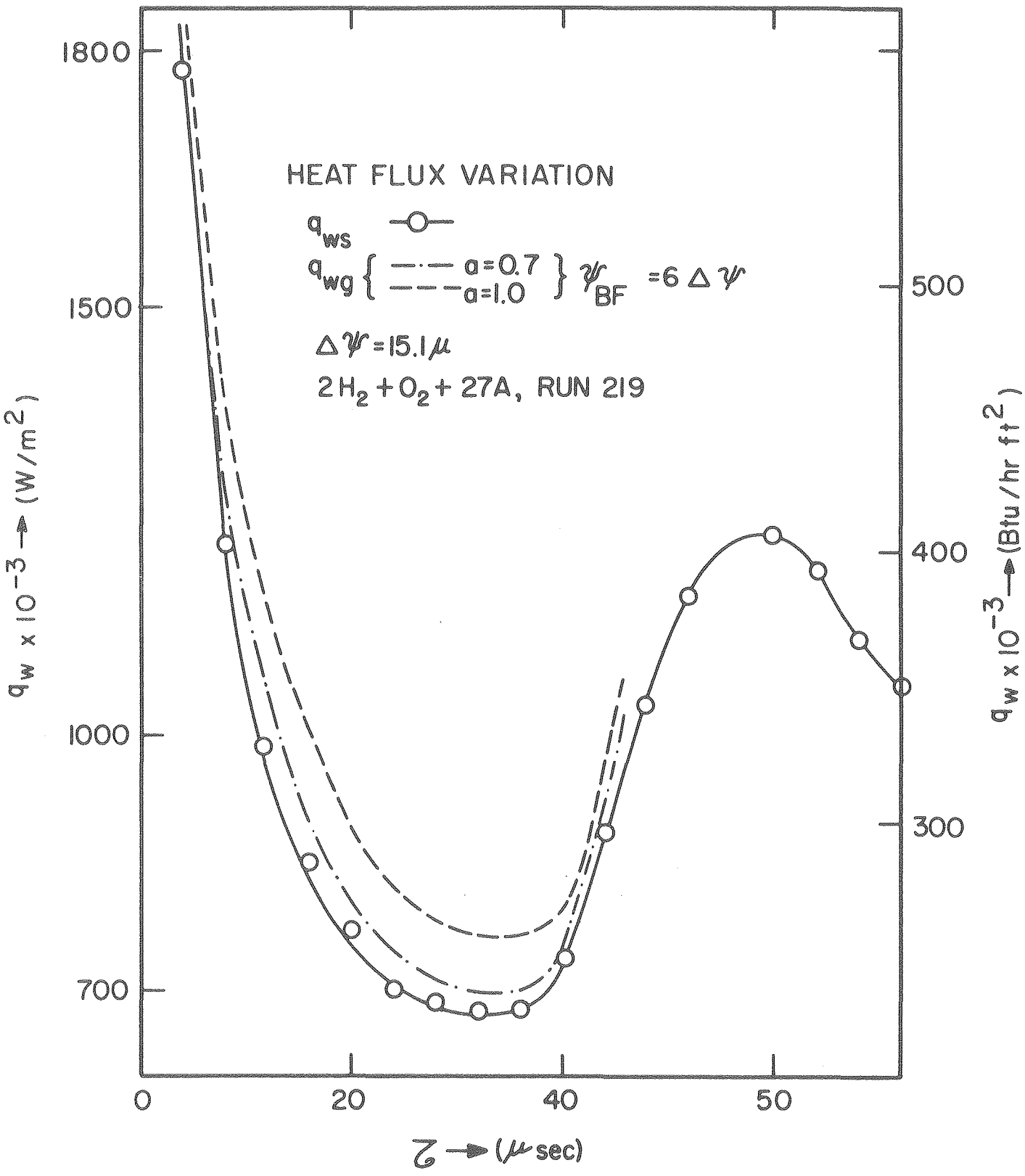


Fig. 8b

XBL806 10304

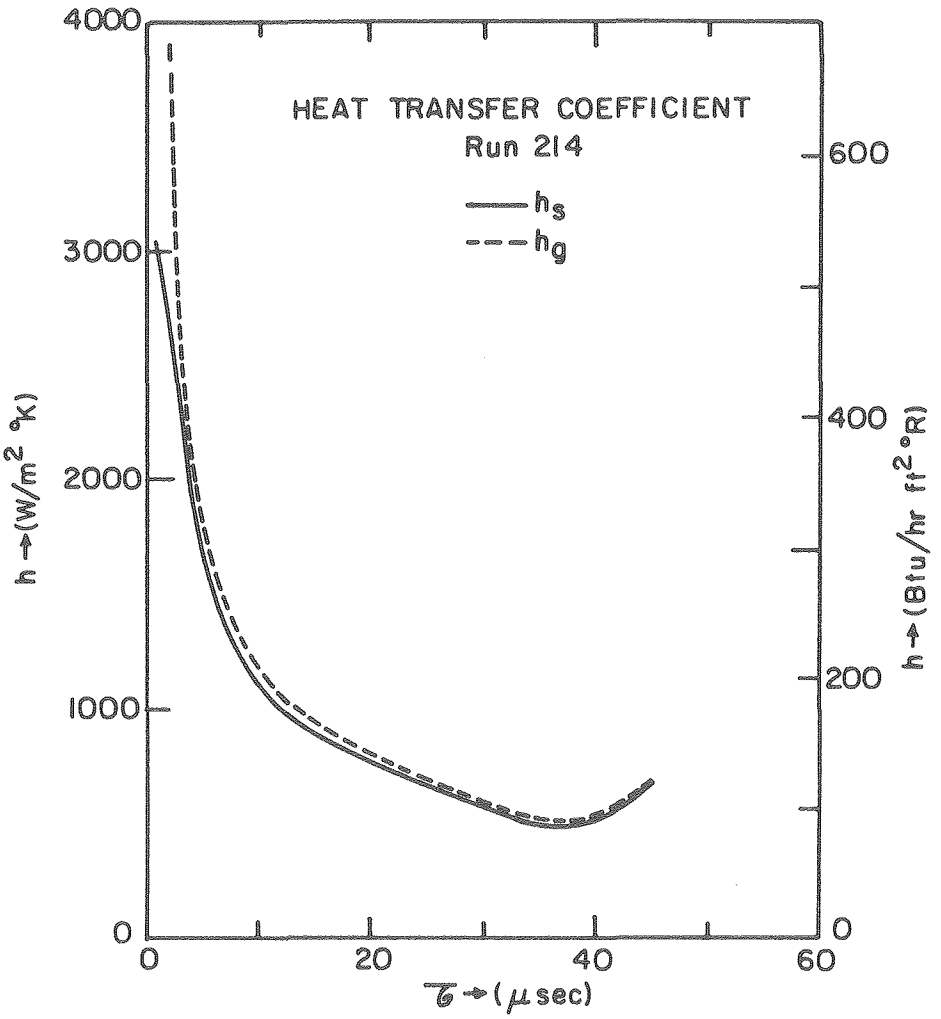


Fig. 9

XBL806 10305

Table 1.

| | RUN 219 | RUN 214 |
|---|---|---|
| τ (μsec) | t(μsec) | t(μsec) |
| 0 | 0 | 0 |
| 10 | 10.0 | 10.0 |
| 20 | 20.0 | 20.0 |
| 21 | 21.0 | 21.0 |
| 22 | 22.0 | 22.0 |
| 23 | 23.0 | 23.0 |
| 24 | 24.0 | 24.0 |
| 25 | 25.0 | 25.0 |
| 26 | 26.0 | 26.0 |
| 27 | 27.0 | 27.0 |
| 28 | 28.0 | 28.0 |
| 29 | 29.0 | 29.0 |
| 30 | 29.9 | 29.9 |
| 31 | 20.9 | 20.9 |
| 32 | 31.9 | 31.9 |
| 33 | 32.8 | 32.8 |
| 34 | 33.8 | 33.8 |
| 35 | 34.7 | 34.7 |
| 36 | 35.7 | 35.7 |
| 37 | 36.6 | 36.6 |
| 38 | 37.5 | 37.5 |
| 39 | 38.5 | 38.5 |
| 40 | 39.4 | 39.4 |
| 41 | 40.3 | 40.3 |
| 42 | 41.2 | 41.2 |
| 43 | 42.1 | 42.1 |
| 44 | 43.0 | 43. |
| 45 | 43.9 | 43.9 |